

PAPER TITLE: Energy Absorption in Chopped Carbon Fiber Compression Molded Composites

AUTHORS: J. Michael Starbuck, George C. Jacob, Srdan Simunovic, Oak Ridge National Laboratory

ABSTRACT

In passenger vehicles the ability to absorb energy due to impact and be survivable for the occupant is called the “crashworthiness” of the structure. To identify and quantify the energy absorbing mechanisms in candidate automotive composite materials, test methodologies were developed for conducting progressive crush tests on composite plate specimens. The test method development and experimental set-up focused on isolating the damage modes associated with the frond formation that occurs in dynamic testing of composite tubes. Quasi-static progressive crush tests were performed on composite plates manufactured from chopped carbon fiber with an epoxy resin system using compression molding techniques. The carbon fiber was Toray T700 and the epoxy resin was YLA RS-35. The effect of various material and test parameters on energy absorption was evaluated by varying the following parameters during testing: fiber volume fraction, fiber length, fiber tow size, specimen width, profile radius, and profile constraint condition. It was demonstrated during testing that the use of a roller constraint directed the crushing process and the load deflection curves were similar to progressive crushing of tubes. Of all the parameters evaluated, the fiber length appeared to be the most critical material parameter, with shorter fibers having a higher specific energy absorption than longer fibers. The combination of material parameters that yielded the highest energy absorbing material was identified.

INTRODUCTION

In passenger vehicles the ability to absorb impact energy and be survivable for the occupant is called the “crash worthiness” of the structure. This absorption of energy is through controlled failure mechanisms and modes that enable the maintenance of a gradual decay in the load profile. The crashworthiness of a material is expressed in terms of its specific energy absorption E_S (SEA) which is

J. Michael Starbuck, Oak Ridge National Laboratory, P.O. Box 2009, Oak Ridge, TN 37831
Srdan Simunovic, Oak Ridge National Laboratory, P.O. Box 2008, Oak Ridge, TN 37831
George C. Jacob, University of Tennessee, Knoxville, 434 Dougherty Eng., Knoxville, TN 37916

characteristic to that particular material. It is defined as the energy absorbed per unit mass of crushed material. Mathematically $E_s = W / (V\rho)$, where the total energy absorbed, W , is calculated by integrating the area under the load-deflection curve, V is the volume of crushed material, and ρ is the density of the material.

In the crashworthiness of automotive structures, the primary issues to the automotive industry are the overall economy and the weight of the material. To reduce the weight and improve the fuel economy, polymer composite materials have replaced more and more metal parts in vehicles. The tailorability of composites, in addition to their attributes of high strength-to-weight and stiffness-to-weight ratios, corrosion resistance and fatigue resistance, makes them very attractive for designing crashworthy structures. The challenge is determining what specific design features are needed in the geometry and what material systems will enable greater safety without negatively affecting the overall economics of fabrication and production.

In comparison to metals, most composites are generally characterized by a brittle rather than ductile response to the applied loads, especially in compression. The major difference, however, is that metal structures collapse under crush or impact by buckling and/or folding in accordion type fashion involving extensive plastic deformation, whereas composites fail through a sequence of fracture mechanisms. The actual mechanisms, e.g., fiber fracture, matrix crazing and cracking, fiber-matrix debonding, delamination, and inter-ply separation, and sequence of damage are highly dependent on lamina orientation, crush speed, triggers and geometry of the structure.

Much of the experimental work to study the effects of fiber type, matrix type, fiber architecture and specimen geometry on the energy absorption of composite materials has been carried out on axisymmetric tubes [1-22]. Tube structures are relatively easy to fabricate and close to the geometry of the actual crashworthy structures. These tubes were designed to absorb impact energy in a controlled manner by providing a trigger to initiate progressive crushing. A trigger is a stress concentrator that causes failure to initiate at a specific location within a structure and propagate through the body in a controlled predictable manner. The most widely used method of triggering is chamfering one end of the tube.

In the progressive crushing of composite tubes there are many different failure mechanisms that contribute to the overall energy absorption of the structure. To isolate the damage mechanisms and quantify the energy absorption contributed by the splaying mode, composite plate specimens were tested using a unique test fixture. Practical considerations related to the cost of production of the test specimens were of paramount importance in developing the test methodology. Composite plate specimens are very cheap to fabricate and it has been observed that plate specimens progressively crush in modes very similar to the damage modes that occur during progressive crushing of composite tubes.

TEST METHOD

A new test fixture design was developed for determining the deformation behavior and damage mechanisms that occur during progressive crushing of

composite materials. The fixture was designed to isolate the damage modes associated with the frond formation (splaying mode) in composite tubes by testing plate geometries. The design of the test fixture can accommodate different plate widths (up to 2 inches), plate thicknesses (nominally $.125 \pm 0.06$ inches), contact profile shapes, and contact profile constraints. The design is a modified version of an existing test fixture used for crush testing of composite plates [23]. Features incorporated into the design include an observable crush zone, long crush length (2 inches), interchangeable contact profile, frictionless roller for contact constraint, and out-of-plane roller supports to prevent buckling. The brackets on each side of the profile plate were designed to provide a method of constraining the specimen to deform along the path of the contact profile. The severity of the contact profile constraint was determined by the position of the brackets and was adjustable using slotted positioning holes. More details of the fixture design are provided by Starbuck, et al, [24].

MATERIAL DESCRIPTION

Through on going research programs a considerable amount of experimental data related to the energy absorption characteristics of polymer composite materials has been generated. For this class of materials the energy absorption is dependent on many parameters including fiber type, matrix type, fiber architecture, specimen geometry, processing conditions, fiber volume fraction, and impact velocity. Changes in these parameters can cause subsequent changes in their specific energy absorption up to a factor of 2. Composite materials are recognized as being efficient energy absorbers, however for a material to be suitable for automotive crashworthy structural applications they must also have low raw material and manufacturing costs. The use of chopped carbon fiber (CCF) and compression molded processing methods has the potential to satisfy these criteria.

Mechanical property and quasi-static progressive crush tests were performed on composite plates manufactured from CCF with an epoxy resin using compression molding techniques. The carbon fiber was Toray T700 and the epoxy resin was YLA RS-35. To investigate the effect of various material parameters there were eight different panel types fabricated where the fiber length, fiber volume fraction, and fiber areal density were varied. The different fiber lengths were 1-inch and 2-inch, the different fiber volume fractions were 40% and 50%, and the areal density was either 150 gsm or 300 gsm. Different areal densities were evaluated as an attempt to study the effect of tow size. The Toray T700 fiber used for the prepreg was a 12K tow but in manufacturing the molding compound the prepreg was slit in addition to cutting the length. The width of the slit was varied to provide the different areal densities.

In addition to the material variables, the effect of certain test parameters on the SEA was considered in the test program. The test parameters were a profile radius of 0.5-inch or 0.25-inch, a profile constraint of none, loose, or tight, and a specimen width of 0.5, 1.0, or 2.0 inches.

MECHANICAL PROPERTIES

Characterization tests were conducted to evaluate the tension, compression, and flexural mechanical properties of the eight different panel types. The tensile strength was evaluated using the ASTM D3039/D 3039M-95a with dog-bone specimen geometry and the strain was measured using an extensometer. Compression strength tests were run per ASTM D3410/D3410M-95 (IITRI Method) and strain gages were used for measuring strains. The flexural strength was determined based on ASTM D790-98 and 4-point loading with a span to depth ratio equal to 16. An LVDT was used for measuring the beam deflection. The test results are summarized in Tables I-III based on a limited sample population (3 specimens per panel type for tension and compression, and 6 specimens for flexure).

Based on the results shown in Tables I-III, some observations from the mechanical property testing are as follows. The smaller the areal density of the CCF the higher the tensile strength and the higher the tensile modulus. Lower tensile strengths and stiffnesses were measured when the chopped fiber length was shorter or when higher fiber volume fractions were used. From the compression tests, the smaller areal density panels had significantly higher compressive strengths and failure strains than the larger areal density panels. The effects of fiber length and fiber volume fraction on compressive strength, stiffness and maximum strain was inconclusive. Consistent with the tension and compression data, the flexure data indicates that testing smaller areal density panels results in higher strengths and stiffnesses. The effect of fiber volume fraction on the flexural response is opposite that of pure tension, where the higher fiber volume fraction tests resulted in higher flexural strengths and stiffnesses. The effect of fiber length was lower flexure strength and higher flexure stiffness when shorter lengths were tested. It should be noted that all of the mechanical properties had tremendous scatter as indicated by the large standard deviations in the tables. This variability in the property data may be indicative of a nonhomogeneous material system and the randomness of the chopped carbon fiber orientation.

TABLE I. CCF TENSILE STRENGTH

Panel Type	ID	Max. Stress (ksi)		Max. Strain (%)		Stiffness (Msi)	
		Avg.	S.D.	Avg.	S.D.	Avg.	S.D.
40% Vf, 1-in., 150 gsm	CCF1	29.4	7.0	0.42	0.05	7.08	1.39
40% Vf, 1-in., 300 gsm	CCF8	23.0	1.2	0.43	0.15	5.49	1.87
40% Vf, 2-in., 150 gsm	CCF2	51.6	9.7	0.58	0.03	9.04	2.14
40% Vf, 2-in., 300 gsm	CCF3	20.8	7.6	0.28	0.12	6.77	0.09
50% Vf, 1-in., 150 gsm	CCF5	28.3	4.7	0.46	0.05	6.06	0.84
50% Vf, 1-in., 300 gsm	CCF9	20.8	3.9	0.48	0.16	4.67	2.38
50% Vf, 2-in., 150 gsm	CCF6	46.4	4.9	0.61	0.06	7.79	0.33
50% Vf, 2-in., 300 gsm	CCF7	23.8	1.9	0.48	0.23	5.26	1.51

TABLE II. CCF COMPRESSIVE STRENGTH

Panel Type	ID	Max. Stress (ksi)		Max. Strain (%)		Stiffness (Msi)	
		Avg.	S.D.	Avg.	S.D.	Avg.	S.D.
40% Vf, 1-in., 150 gsm	CCF1	47.1	4.6	1.23	0.17	5.29	0.85
40% Vf, 1-in., 300 gsm	CCF8	30.0	3.0	0.77	0.24	4.96	0.72
40% Vf, 2-in., 150 gsm	CCF2	44.4	2.2	1.45	0.26	3.89	0.74
40% Vf, 2-in., 300 gsm	CCF3	36.2	1.4	0.70	0.04	5.70	0.05
50% Vf, 1-in., 150 gsm	CCF5	34.3	1.9	1.31	0.21	3.62	0.36
50% Vf, 1-in., 300 gsm	CCF9	27.9	4.4	0.65	0.41	5.44	2.10
50% Vf, 2-in., 150 gsm	CCF6	53.2	4.3	1.13	0.03	5.45	0.75
50% Vf, 2-in., 300 gsm	CCF7	32.0	6.1	0.80	0.19	4.78	1.73

TABLE III. CCF 4-POINT FLEXURE STRENGTH

Panel Type	ID	Max. Stress (ksi)		Max. Strain (%)		Stiffness (Msi)	
		Avg.	S.D.	Avg.	S.D.	Avg.	S.D.
40% Vf, 1-in., 150 gsm	CCF1	46.1	8.0	1.84	0.20	0.70	0.07
40% Vf, 1-in., 300 gsm	CCF8	30.5	6.1	1.51	0.32	0.60	0.07
40% Vf, 2-in., 150 gsm	CCF2	58.1	10.5	2.10	0.12	0.67	0.06
40% Vf, 2-in., 300 gsm	CCF3	37.8	9.9	1.63	0.26	0.58	0.14
50% Vf, 1-in., 150 gsm	CCF5	49.7	7.1	1.52	0.16	0.80	0.10
50% Vf, 1-in., 300 gsm	CCF9	38.2	6.5	1.33	0.34	0.76	0.11
50% Vf, 2-in., 150 gsm	CCF6	71.0	10.8	1.91	0.15	0.73	0.06
50% Vf, 2-in., 300 gsm	CCF7	36.9	5.3	1.70	0.30	0.56	0.05

PROGRESSIVE CRUSH

Testing Procedure

The CCF specimen had a nominal length of 7 inches and a 45° chamfer was used as the crush initiator. A diamond cut off wheel was used to cut the specimens off the composite panel. No coolant was used during cutting to prevent contamination of the test specimens. In some of the tests a metal push plate needed to be used to reduce the unsupported specimen length. This metal push plate was 3 inches in length and was bonded to the end of the test specimen using 5-minute epoxy. This called for the test specimens to be trimmed to a length of 4 inches so that it could accommodate the metal push plate. A servo-hydraulic test machine and a loading rate of 0.2 inches/min were used throughout the entire testing. The load-deflection response was recorded using a computerized data acquisition system. The area under the load deflection curve was calculated for the total energy absorbed and the initial peak load and sustained crush load were identified.

Results and Discussion

For all specimens tested, local crushing took place at the chamfered end of the plates. Matrix cracking occurred at the ends of the fiber tows due to stress concentration at these ends, followed by fiber-matrix debonding in the majority of specimens tested. The damage process appeared to be controlled by the flexural deformations taking place as the specimen was pushed through the profile radius.

Some of the test specimens when loaded in the no constraint condition experienced fiber pull out, fiber breakage on the tension side and fiber buckling on the compression side of the specimen. The fracture mechanisms that took place in specimens crushed under the loose and tight constraint condition were repeatable over the entire test matrix and the specimen failure was more or less predictable. On the contrary, specimens that were crushed in the no constraint condition fractured in rather erratic fashions and specimen failure was far less predictable. This was due to absence of the much needed roller constraint required to direct the crushing process. Some of the no constraint tests lead to catastrophic failure of the specimen where in the specimen broke in to 2 or 3 pieces.

The specimens tested in the loose and tight constraint conditions generated load deflection curves that were similar to the ones generated during the progressive crushing of composite tubes. There were 4 stages, the first one being characterized by an initial rapid load increase. A rapid load drop occurred in the second stage of the load deflection curve followed by a gradual saturation of the load. The final stage was characterized by stable crushing at a constant mean load (see Figure 1). The small load fluctuations and serrations in the fourth stage of the curve are characteristic of stable crushing.

EFFECT OF TOW SIZE

The effect of areal density or tow size was determined by comparing panel groups CCF5 to CCF9 and CCF1 to CCF8 (reference Tables I-III for panel descriptions). The specific energy absorption of CCF5 was found to be greater than CCF9 and CCF1 was greater than CCF8. Figure 2 shows a comparison of the load displacement traces recorded for a test conducted on a specimen belonging to panel group CCF5 and on a specimen belonging to panel group CCF9.

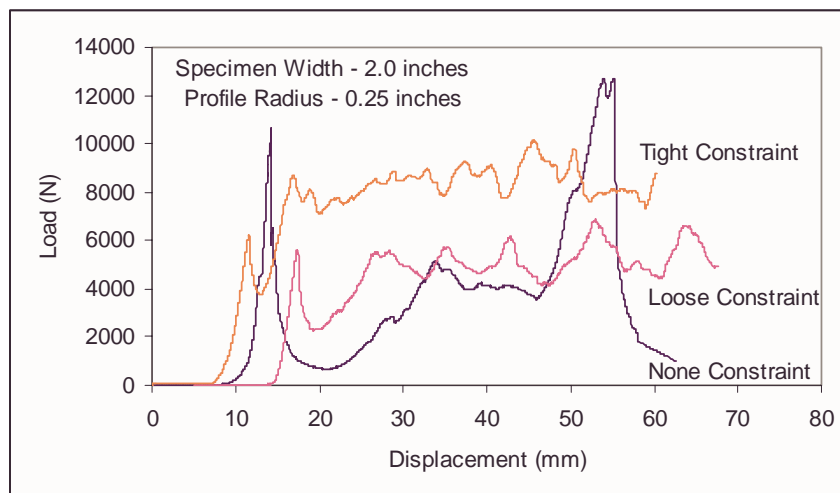


Figure 1. Load displacement traces for CCF.

Hence it was concluded that an increase in tow size caused a decrease in the specific energy absorption for chopped carbon fiber composite materials with 1-inch fiber length. However, the trends in the data were not as consistent for the 2-inch fiber length, and it was concluded that there was no serious effect of tow-size for the longer fiber length.

EFFECT OF FIBER VOLUME FRACTION

On comparing panel group CCF2 and panel group CCF6, the specific energy absorption of CCF2 was found to be greater than that of CCF6. Panel group CCF3 and panel group CCF7 was also compared and it was found that the specific energy absorption of CCF3 was greater than that of CCF7. For a comparison of the load displacement traces recorded for a test conducted on a specimen belonging to panel group CCF3 and on a specimen belonging to panel group CCF7 see Figure 3. Based on these results, it was concluded that an increase in fiber volume fraction caused a decrease in the specific energy absorption for chopped carbon fiber composite materials with fiber length of 2 inches. However, comparing panel group CCF5 and panel group CCF1 the specific energy absorption of CCF5 was greater than that of CCF1. Figure 4 compares the load displacement traces recorded for a test conducted on a CCF5 specimen and on a CCF1 specimen. Based on this data it was concluded that an increase in fiber volume fraction caused an increase in the specific energy absorption for chopped carbon fiber composite materials with 1-inch fiber length.

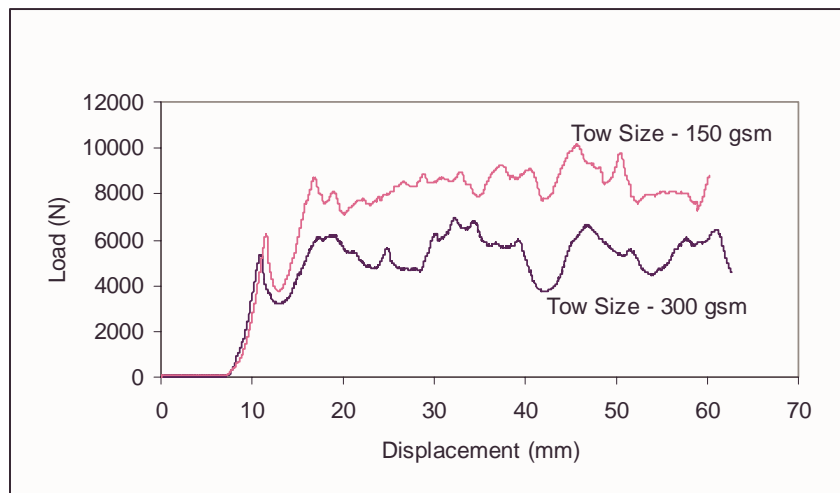


Figure 2. Load displacement traces representing the effects of tow size on the SEA of CCF with 1-inch fiber length.

EFFECT OF FIBER LENGTH

On comparing panel group CCF5 and panel group CCF6, the specific energy absorption of CCF5 was found to be greater than that of CCF6. For a comparison of the load displacement traces recorded for a test conducted on a specimen belonging to panel group CCF5 and on a specimen belonging to panel group CCF6 please see Figure 5. Panel group CCF1 and panel group CCF2 was also compared and it was found that the specific energy absorption of CCF1 was greater than that of CCF2. Comparing panel group CCF9 and panel group CCF7 showed the specific energy absorption of CCF9 to be greater than that of CCF7. Therefore, it was concluded that an increase in fiber length caused a decrease in the specific energy absorption for chopped carbon fiber composite materials.

Previous studies on the effect of fiber length on the energy absorption capabilities of composite plates have reported an increase in the SEA with increased fiber lengths [25]. The effect of fiber length on SEA observed in this work disagrees with this conclusion. It is speculated that this could be a result of many factors, including the microstructure of the material system, manufacturing process, specimen geometry, and/or test methodology.

EFFECT OF PROFILE RADIUS

In all the tests performed on chopped carbon fiber composite materials, irrespective of the specimen width or the constraint condition, an increase in the profile radius caused a decrease in the specific energy absorption, SEA. For a comparison of the load displacement traces recorded for a test conducted on a specimen using a profile block of radius 0.25 inches and on a specimen using a profile block of radius 0.5 inches see Figure 6.

The decrease in SEA with an increase in the profile radius is due to the fact that a specimen loaded in compression is crushed through the contact profile as defined by the profile block. When a larger radius is used the specimen follows a smoother curve that requires less axial load to produce the flexural deformations. Therefore, less energy is absorbed during the progressive crush test.

EFFECT OF SPECIMEN WIDTH

In all the tests conducted, irrespective of the constraint condition or the radius of the profile block, the 2-inch wide specimens displayed the highest specific energy absorption followed by either the 1-inch or the 0.5-inch wide specimens. Figure 7 shows a comparison of the load displacement traces recorded for specimens having 0.5-inch, 1-inch and 2-inch widths. The reason for the greater energy absorption in the 2-inch wide specimens was due to the fiber lengths being less than or equal to the width of the specimen. For the 0.5- and 1-inch wide specimens the fiber lengths were greater than the width of the specimen. This results in fewer fiber ends for the narrower specimens and consequently, fewer fracture initiation sites.

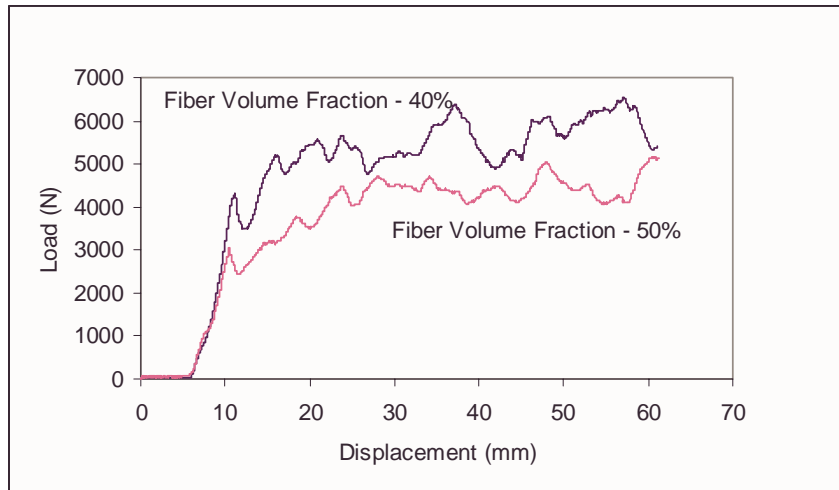


Figure 3. Load displacement traces representing the effect of fiber volume fraction on the SEA of CCF with 2-inch fiber length.

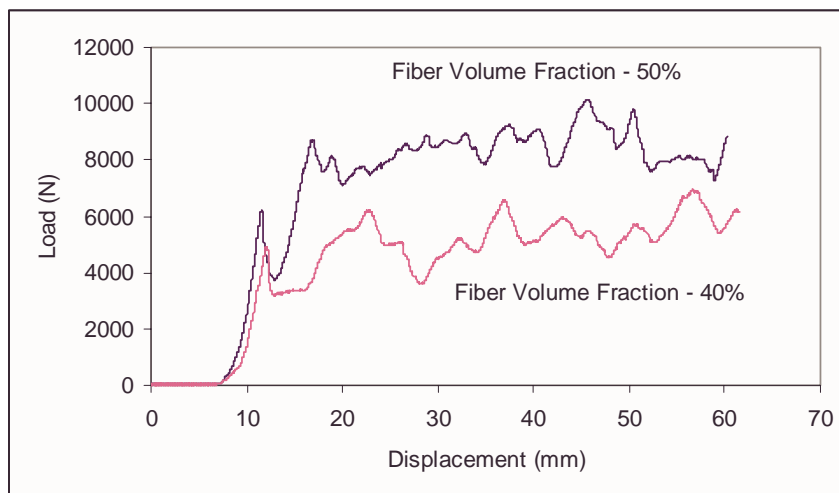


Figure 4. Load displacement traces representing the effect of fiber volume fraction on the SEA of CCF with 1-inch fiber length.

EFFECT OF CONSTRAINT

The tests conducted on the CCF material were only successful when the roller was positioned in the tight and loose constraint condition. When the no constraint condition was attempted the initial peak load increased and the CCF specimens buckled between the top plate and roller ways. The roller ways were unsuccessful in preventing out-of-plane buckling in the CCF material because of its low buckling strength. This resulted in having to use a metal push plate to reduce the unsupported specimen length. Using this modified specimen configuration the no constraint condition resulted in the highest initial peak load relative to the other constraint

conditions. Comparing the SEA's, the lowest SEA corresponded to the no constraint condition when compared to either tight or loose constraint condition. For a comparison of the load displacement traces recorded for a test conducted on a specimen in the no constraint, the loose constraint and the tight constraint condition see Figure 1.

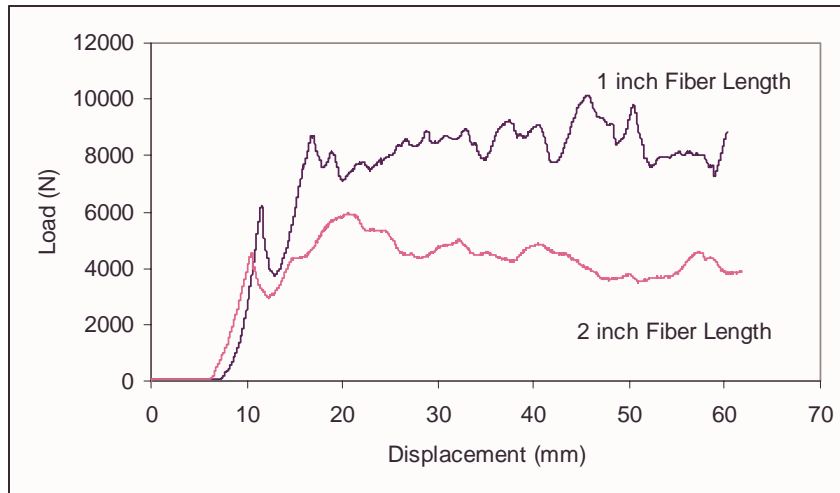


Figure 5. Load displacement traces representing the effect of fiber length on the SEA of CCF with 150-gsm areal density.

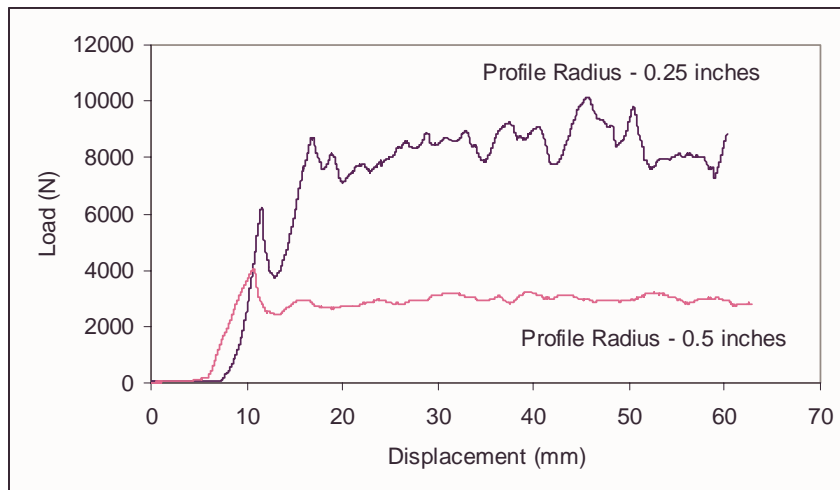


Figure 6. Load displacement traces representing the effect of profile radius on the SEA of CCF.

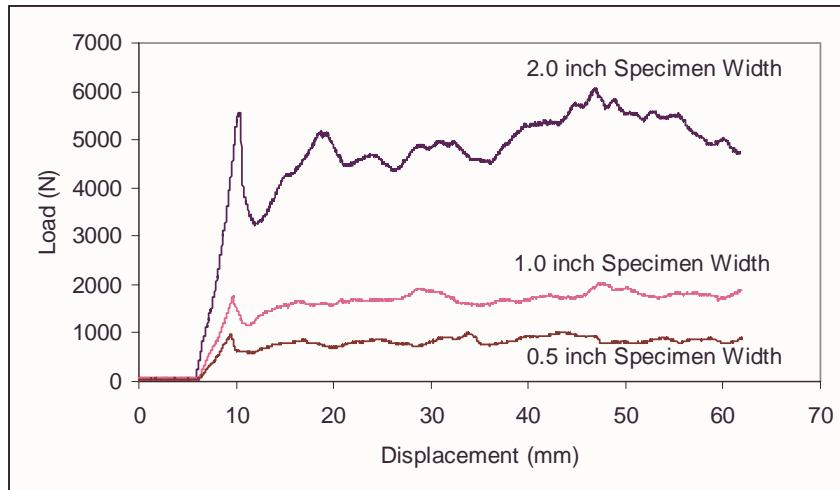


Figure 7. Load displacement traces representing the effect of specimen width on the SEA of CCF.

SUMMARY

Quasi-static progressive crush strip tests were conducted on randomly oriented CCF composite materials to evaluate their energy absorption capability. The objective of the test method was to simulate the frond formation observed during dynamic crush tests of composite tubes. The test program considered three material parameters, fiber length, fiber volume fraction, and areal density; and three test parameters, specimen width, profile radius, and profile constraint. Eight different types of panels were fabricated and tested, and the panel group having the highest SEA (CCF5) corresponded to 50% fiber volume fraction, 1-inch fiber length, and 150-gsm areal density. The 2 panel groups that recorded the lowest SEA were CCF6 and CCF7. This indicates that it is the 2-inch long fibers causing the SEA of the CCF6 and CCF7 panel groups to be the least among all the other CCF panel groups. Figure 6 showed the effect that longer fiber lengths had on SEA was a decrease relative to the shorter fiber lengths. Therefore, it appears from this study that the fiber length is the most critical material parameter in determining the SEA of a composite material, with shorter fiber lengths leading to higher SEAs'. The damage process appeared to be controlled by the flexural deformations. Based on the mechanical property tests, the highest SEA system corresponded to a CCF material system having high flexural stiffness but low flexural strength properties.

ACKNOWLEDGEMENT

The U.S. Department of Energy, Assistant Secretary for Energy Efficiency and Renewable Energy, Office of Transportation Technologies, Lightweight Materials Program, sponsored this research under contract DE-AC05-00OR22725 with UT-Battelle, LLC.

REFERENCES

1. Thornton, P. H. and P. J. Edwards. 1982. "Energy Absorption in Composite Tubes," *J. Comp. Mat.*, 16:521-545.
2. Schmuesser, D. W. and L. E. Wickliffe. 1987. "Impact Energy Absorption of Continuous Fiber Composite Tubes," *J. Engng. Mat. & Tech.*, 109:72-77.
3. Farley, G. L. 1987. "Energy Absorption of Composite Material and Structures," Proc. 43rd American Helicopter Society Annual Forum, St. Louis, Missouri, pp. 613-627.
4. Farley, G. L. 1986. "Effect of Specimen Geometry on the Energy Absorption Capability of Composite Materials," *J. Comp. Mat.*, 20:390-400.
5. Farley, G. L. 1983. "Energy Absorption of Composite Materials," *J. Comp. Mat.*, 17:267-279.
6. Farley, G. L. 1986. "Effect of Fiber and Matrix Maximum Strain on the Energy Absorption of Composite Materials," *J. Comp. Mat.*, 20:322-334.
7. Farley, G. L. 1987. "Energy Absorption in Composite Materials for Crashworthy Structures," Proc. Of ICCM6, Elsevier Science Publishers, London, pp. 3.57-3.66.
8. Hull, D. 1991. "A Unified Approach to Progressive Crushing of Fiber Reinforced Composite Tubes," *Comp. Sci. Technol.*, 40:377-421.
9. Hull, D. 1983. "Axial Crushing of Fibre Reinforced Composite Tubes," in *Structural Crashworthiness*, N. Jones and T. Weirzbicki, Butterworths, London, pp. 118-135.
10. Hamada, H., S. Ramakrishna, Z. Maekawa, and M. Nakamura. 1994. "Energy Absorption Behavior of Hybrid Composite Tubes," Proc. 10th Annual ASM/ESD Advanced Composite Conference, Dearborn, Michigan, pp. 511-522.
11. Hamada, H. and S. Ramakrishna. 1996. "Effect of Fiber Material on the Energy Absorption Behavior of Thermoplastic Composite Tubes," *J. Thermo. Comp. Mat.*, 9(3):259-279.
12. Farley, G. L. and R. M. Jones. 1992. "Analogy for the Effect of Material and Geometrical Variables on Energy Absorption Capability of Composite Tubes," *J. Comp. Mat.*, 26(1):78-89
13. Thornton, P. H. 1979. "Energy Absorption in Composite Structures," *J. Comp. Mat.*, 13:247-262.
14. Ramakrishna, S., H. Hamada, Z. Maekawa, and H. Sato. 1995. "Energy Absorption Behavior of Carbon Fiber Reinforced Thermoplastic Composite Tubes," *J. Thermo. Comp. Mat.*, 8:323-344.
15. Farley, G. L. 1986. "Crash Energy Absorbing Composite Sub-floor Structure," 27th SDM Conference, May 1986.
16. Ramakrishna, S. and D. Hull. 1993. "Energy Absorption Capability of Epoxy Composite Tubes with Knitted Carbon Fibre Fabric Reinforcement," *Comp. Sci. Technol.*, 49:349-356.
17. Ramakrishna, S. 1992. "Knitted Fabric Reinforced Polymer Composites," Ph.D. Thesis, University of Cambridge, UK.
18. Ramakrishna, S. 1995. "Energy Absorption Characteristics of Knitted Fabric Reinforced Composite Tubes," *J. Reinf. Plast. & Comp.*, 14:1121-1141.
19. Ramakrishna, S., H. Hamada, and D. Hull. 1995. *Impact and Dynamic Fracture of Polymers and Composites*, (ESIS10), Mechanical Engineering Publications, London, pp. 453-464.
20. Ramakrishna, S. and D. Hull. 1990. Proc. International Conference on Advances in Structural Testing, Analysis, and Design, McGraw-Hill, pp. 69-74.
21. Hamada, H., S. Ramakrishna, Z. Maekawa, and M. Nakamura. 1994. "Energy Absorption Characteristics of Composite Tubes with Different Cross Sectional Shapes," Proc. 10th Annual ASM/ESD Advanced Composite Conference, Dearborn, Michigan, pp. 523-534.
22. Hamada, H., A. Nakai, and T. Nakatani. 1996. "Energy Absorption Properties of Braided I-beam," Proc. Joint Canada-Japan Workshop on Composites, Kyoto, Japan, pp. 277-280.
23. Lavoie, J. A. and J. Morton. 1993. "Design and Application of a Quasistatic Crush Test Fixture for Investigating Scale Effects in Energy Absorbing Composite Plates," NASA Contractor Report 4526, July 1993.
24. Starbuck, J. M., G. C. Jacob, and S. Simunovic. 2000. "Test Methodologies for Determining Energy Absorbing Mechanisms of Automotive Composite Material Systems," Doc. No. 2000-01-1575, Future Car Congress, Crystal City, VA, USA, April 2000.
25. Snowdon, P. and D. Hull. 1984. "Energy Absorption of SMC Under Crash Conditions," Proc. Fiber Reinforced Composites Conference '84, Plastics and Rubber Institute, 3rd-5th April, 1984 pp. 5.1-5.10.